Electronic Supplementary Information (ESI)

The role of nanoparticle charge in crystallization kinetics and ice adhesion strength for dispersions of detonation nanodiamonds

Alexandre M. Emelyanenko,* Kirill A. Emelyanenko, Alexander Ya. Vul', Alexander V. Shvidchenko and Ludmila B. Boinovich*

A.N. Frumkin Institute of Physical Chemistry and Electrochemistry, Russian Academy of Sciences, Moscow, Russia

### Preparation of hydrosols with positively and negatively charged detonation nanodiamonds

Industrial detonation nanodiamond (DND) powder produced by Special Design and Technology Bureau "Technolog" (St. Petersburg, Russia) was used. Purification of DND powder from metal and inert impurities was carried out by sequential etching in HCl and HF with multiple washing in deionized water by centrifugation.

Following the procedures elaborated in detail earlier,[S1] the annealing of purified DND powder was carried out by heating in hydrogen at 700°C for 3 h and in the air at 410°C for 6 h to obtain DND particles with positive and negative ζ-potentials in water, respectively.

Hydrosols of investigated samples were prepared by ultrasonic dispersion of annealed powders in deionized water followed by centrifugation. The dispersion frequency and duration were 22 kHz and 15 min, specific energy absorbed by the hydrosol was 600 J/g. The centrifugation was performed with a relative centrifugal force of 1.8×10^4 g (where g is the gravitational acceleration) and duration of 40 min for the separation of individual DND particles with an average size of 4.5 nm (Figure S1c,d) from the remaining aggregates (Figure S1a,b). The hydrosols were diluted with deionized water to reach a particle concentration of 0.7 wt.%. Obtained hydrosols of individual DND particles with positive (DND$^+$) and negative (DND$^-$) ζ-potentials were used for experiments.
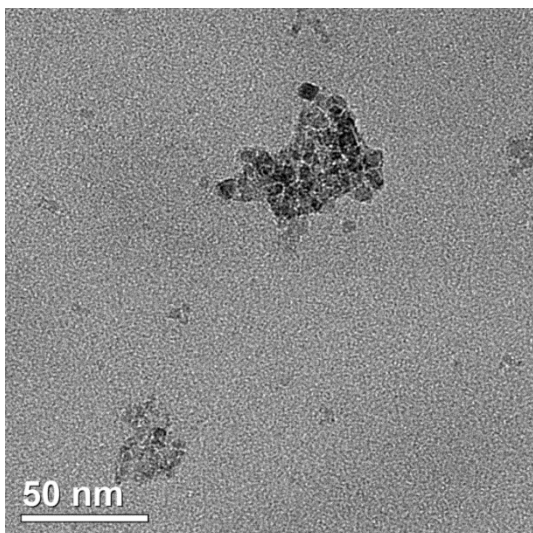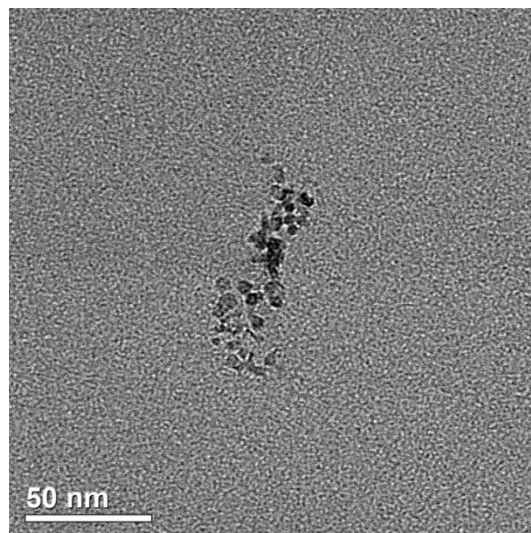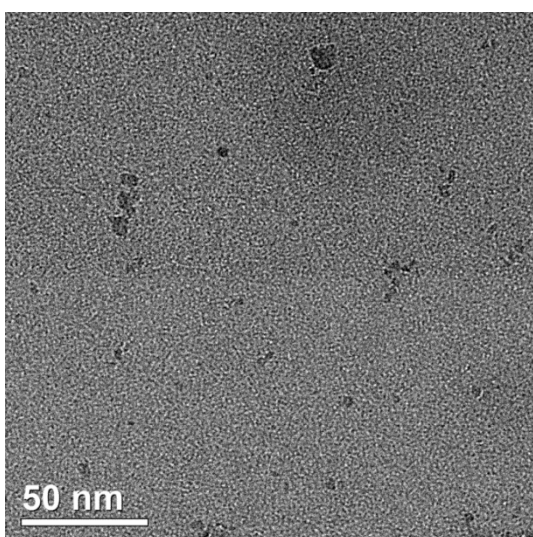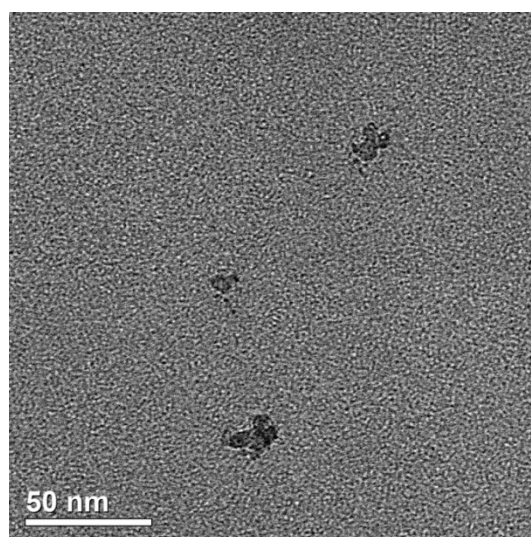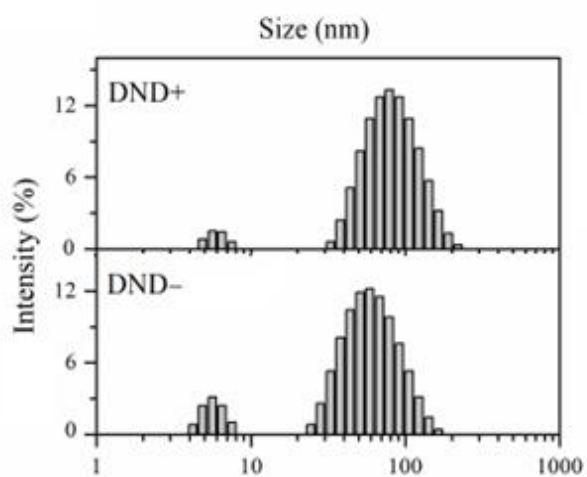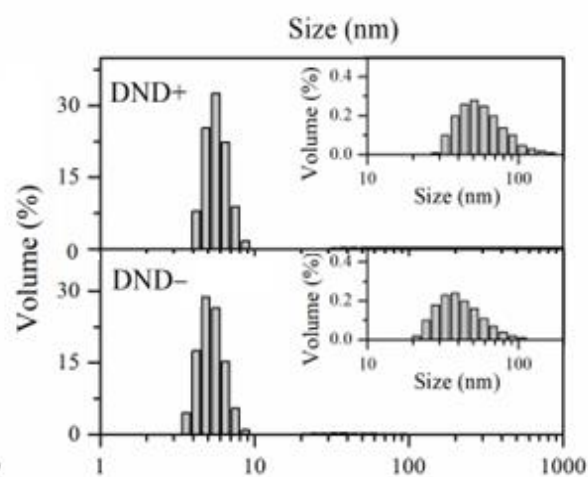
Figure S1. TEM images of positively (a,c) and negatively (b,d) charged detonation nanodiamonds before (a,b) and after (c,d) centrifugal separation; (e,f) Size distributions of DND^+ and DND^- particles by intensity (e) and by volume (f) in dispersions after centrifugal separation.
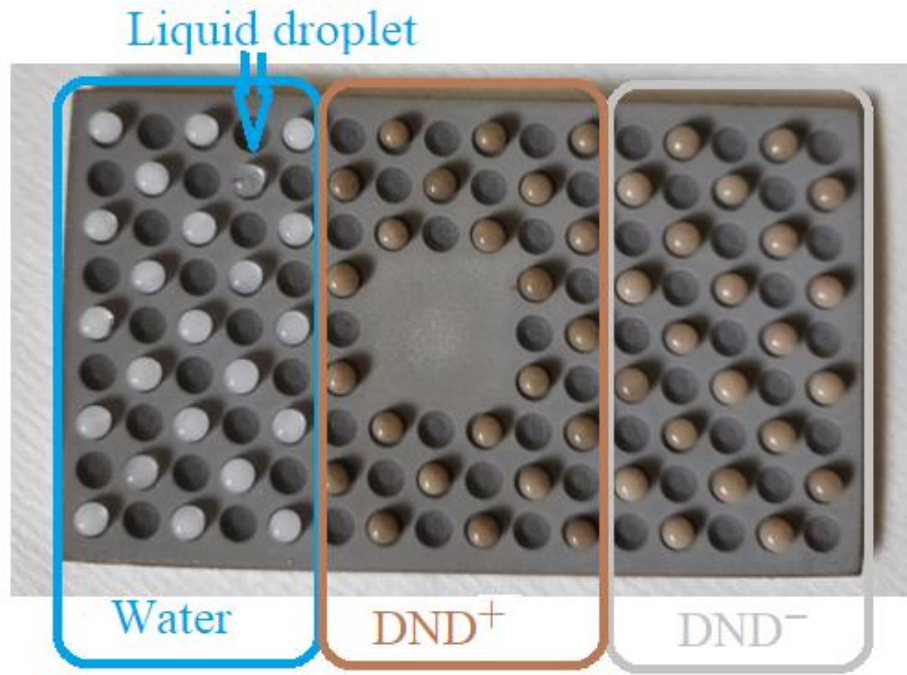
Figure S2. The superhydrophobic substrate with dimples for conveniently placing the test droplets for the study of crystallization statistics. In this image, all droplets but one water droplet are already crystallized.

The analysis of van der Waals interactions between the diamond particles and the superhydrophobic substrate

The van der Waals and electrostatic forces which are determining for the adhesion of liquid or ice to the substrate significantly depend on the structure of the surface layer. For nanodispersions interacting with a substrate, the distribution of the nanoparticles in vicinity of interface is playing a crucial role. Here we estimate the value of the van der Waals interaction between the diamond nanoparticles and the superhydrophobic substrate. The sketch of the considered system is presented in Fig. S3.

Liquid dispersion of detonation nanodiamond (DND) particles in water interacts with a superhydrophobic alumina surface through the layer of a hydrophobic agent (fluorooxysilane). The thickness of the fluorooxysilane layer is of order of 1 nm.[S2]

The energy of the van der Waals interaction, U_{vdW}, between the nanoparticle and the semi-infinite body through the water interlayer with thickness δ can be calculated using the equation[S3]

$$U_{vdW}(\delta) = \frac{-3k_B T v_{DND}}{8\pi\delta^3} \sum_{N=0}^{\infty} \frac{\varepsilon_{DND}(i\xi_N) - \varepsilon_w(i\xi_N)}{\varepsilon_{DND}(i\xi_N) + 2\varepsilon_w(i\xi_N)} \frac{\varepsilon_{substrate}(i\xi_N) - \varepsilon_w(i\xi_N)}{\varepsilon_{substrate}(i\xi_N) + \varepsilon_w(i\xi_N)} = -A/\delta^3, \tag{S1}$$

where k_B is the Boltzmann constant; T is temperature; N is a natural number corresponding to the current summation term; v_{DND} is the DND particle volume; $\xi_N = 2\pi k_B TN/\hbar$; $\hbar$ is the Planck constant; $\epsilon(i\xi_N)$ is the imaginary frequency ($i\xi$) dependence of dielectric permittivity of water (index w), DND particles (*DND*) and the substrate, and δ is a distance between a particle and a substrate.
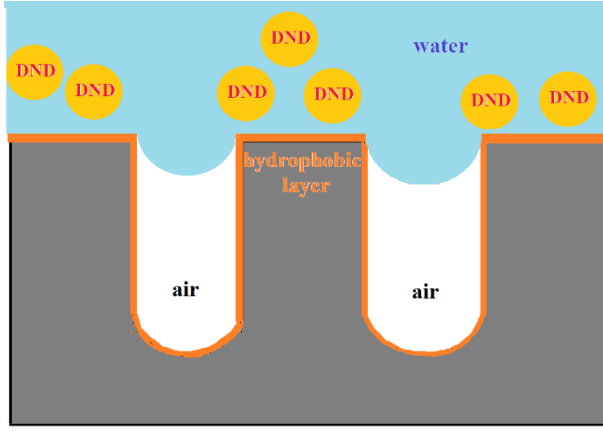
3

Fig. S3. The scheme illustrating the distribution of detonation nanodiamond (DND) particles in the water phase in the vicinity of interface with the superhydrophobic substrate.

Earlier it was shown (see the discussion in ref. S4) that for a composite substrate obtained by the deposition of a thin layer with the dielectric properties different from the properties of the underlying bulk substrate, one can use the effective substrate characteristics to calculate the energy of the van der Waals interaction between the nanoparticle and the substrate. When the distance between the particle and the substrate is of the order of the thickness of upper layer, the approximation of the properties of the effective substrate by the properties of the upper layer will be reliable enough.

In contrast, for the distances between the particle and the composite substrate notably higher than the thickness of the upper layer, one can use the approximation of the properties of the effective substrate by the properties of the bulk substrate. Having in mind the abovementioned arguments, we have calculated the values of the interaction constant A for the cases, when the dielectric response of the composite substrate is modelled by the properties of the layer of fluorooxysilane ($A_{DND/water/fluoro}$), by the alumina properties ($A_{DND/water/Al2O3}$) and by considering air as a substrate ($A_{DND/water/air}$).

To perform the calculations of dielectric permittivity of contacting bodies, in the Eq. (S1) for the fluorooxysilane layer and for DND particles we have adopted two-oscillator model suggested by Ninham and Parsegian:[S5]

$$\varepsilon(i\xi) = 1 + \frac{C_{IR}}{1 + (\xi/\omega_{IR})^2} + \frac{C_{UV}}{1 + (\xi/\omega_{UV})^2}$$

For dielectric spectra of Al_2O_3 we have used the model, suggested by Gudarzi and Aboutalebi:[S6]

$$\varepsilon(i\xi) = 1 + \frac{C_{IR}}{1 + (\xi/\omega_{IR})^2} + \frac{C_{UV}}{1 + (\xi/\omega_{UV})^{1.73}}$$

And for the water we have adopted the three-oscillator model:[S4,S5]

$$\varepsilon(i\xi) = 1 + \frac{C_{\text{IR}}}{1 + (\xi/\omega_{\text{IR}})^2} + \frac{C_{\text{UV}}}{1 + (\xi/\omega_{\text{UV}})^2} + \frac{C_{\text{M}}}{1 + (\xi/\omega_{\text{M}})^2}$$

Exact values used in calculation and references to the value source are listed in the Table S1.

The behavior of the calculated dielectric permittivity of the considered media as a function of the imaginary frequency is shown in Fig. S4, while the calculated constants are presented in the Table S2.

Table S1. Parameters of oscillators used to calculate the dielectric permittivity of contacting media.

Material	C_{IR}	C_{UV}	C_M	ω_{IR}	ω_{UV}	ω_M	Reference
Al_2O_3	6.95	2.08	-	9.22×10^{13}	2.14×10^{16}	-	[S6]
Fluorooxysilane*	0.25	0.846	-	2.27×10^{14}	1.79×10^{16}	-	[S7]
Water	3.846	0.754	74.61	9.70×10^{13}	1.858×10^{16}	1.088×10^{11}	[S8]
Diamond	0.02	4.642	-	2.5×10^{14}	1.61×10^{16}		[S9]

*The dielectric properties of the fluorooxysilane were accepted the same as for PTFE.
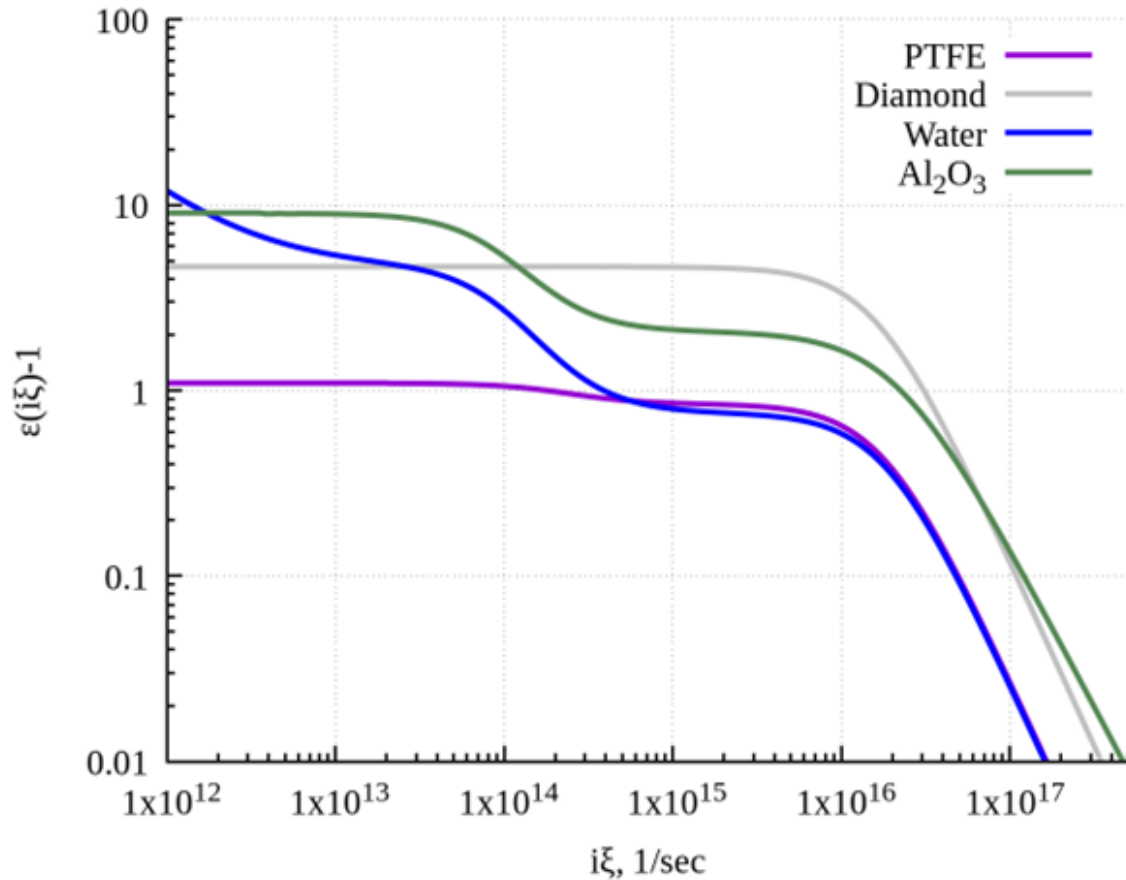

Fig. S4. The behavior of the calculated dielectric permittivities of the considered media as a function of the imaginary frequency

Table S2. Calculated constants A in Eq. (S1.)

System	Constant A, J m^3
DND/water/fluorooxysilane	1.9×10^{-47}
DND/water/Al2O3	2.8×10^{-46}
DND/water/air	-2.0×10^{-46}

Having in mind that the positive sign of the constant A corresponds to the van der Waals attraction of DND particle to the substrate, while negative constant A is associated to repulsion, one can conclude that the concentration of DND nanoparticles will be enhanced near the tops of the elements of texture in comparison to the bulk water. In contrast, in the areas of air bubbles captured inside the texture, the concentration of DND will be less than in the bulk dispersion.

References

S1 A. T. Dideikin, A. E. Aleksenskii, M. V. Baidakova, P. N. Brunkov, M. Brzhezinskaya, V. Y. Davydov and A. Y. Vul', Rehybridization of Carbon on Facets of Detonation Diamond Nanocrystals and Forming Hydrosols of Individual Particles, *Carbon*, 2017, **122**, 737–745. https://doi.org/10.1016/j.carbon.2017.07.013

S2. L. B. Boinovich, A. M. Emelyanenko, V.V. Korolev and A.S. Pashinin, Effect of Wettability on Sessile Drop Freezing. When the Superhydrophobicity Stimulates Extreme Freezing Delay, Langmuir, 2014, 30 (6), 1659–1668. https://doi.org/10.1021/la403796g

S3. Derjaguin, B.V.; Dzyaloshinsky, I.E.; Koptelova M.M.; Pitaevsky L.P. Molecular-surface forces in binary solutions. Faraday Discuss. 1965, 40, 246–252.

S4. Derjaguin, B.V.; Churaev, N.V.; Muller, V.M. Surface Forces, Publisher: Consultants Bureau, USA, 1987.

S5. B. W. Ninham and V. A. Parsegian, van der Waals Forces across Triple-Layer Films, J. Chem. Phys. 1970, 52(9), 4578–4587. https://doi.org/10.1063/1.1673689

S6. M. M. Gudarzi and S. H. Aboutalebi, Self-Consistent Dielectric Functions of Materials: Toward Accurate Computation of Casimir – van der Waals Forces, Sci. Adv. 2021, 7(22), eabg2272. https://doi.org/10.1126/sciadv.abg2272

S7. D. B. Hough and L. R. White, The Calculation of Hamaker Constants from Lifshitz Theory with Applications to Wetting Phenomena, Adv Colloid Interface Sci. 1980, 14(1), 3–41. https://doi.org/10.1016/0001-8686(80)80006-6

S8. L. B. Boinovich and A.M. Emelyanenko, Wetting behaviour and wetting transitions of alkanes on aqueous surfaces, Advances in Colloid and Interface Science, 2009, 147, 44–55. https://doi.org/10.1016/j.cis.2008.10.007

S9. Bergström L. Hamaker constants of inorganic materials, Advances in colloid and interface science, 1997, 70, 125-69. https://doi.org/10.1016/S0001-8686(97)00003-1